

WIDE AREA MULTILATERATION SIMULATION

J. F. Alonso¹, C. Benavente²

¹ISAA, ²ICS Department
Universidad Politécnica de Madrid
Madrid, Spain

¹josefelix.alonso@upm.es, ²cesar.benavente@upm.es

Abstract— Nowadays, multilateration systems based on SSR (Secondary Surveillance Radar) transponder signals are being developed and implanted, due to two factors mainly: the signal processing speed and the system's low cost. In this way, Airport Surface Primary Radars are being replaced by MLAT (Multilateration) systems in surrounding airport areas, and SSR systems by WAM (Wide Area Multilateration) systems for surveillance purposes. The aim of a multilateration surveillance system is to provide, in real-time, the position and indicatives of any aircraft or vehicle equipped with an SSR transponder. To these purposes, the system must be able to measure, with the highest precision, the time difference of arrival (TDOA) of the signal transmitted by the aircraft's transponder to a pair of ground receivers and decode the squawk or S code from the transponder responses. This document presents a software tool to analyze system performance based on the stations' geometry, architecture and receiver type or TDOA algorithms.

I. INTRODUCTION

In order to analyze multilateration systems performances a simulation platform has been developed, although the initial tool has been oriented to the WAM systems analysis, actually different modules needed to implement MLAT systems are being developed like an scenario builder, a signal visibility module improvement or a new signal detection module for multipath environments. Through the use of this tool different architectures and algorithms for signal detection can be analyzed, as well as signal processing algorithms and the solution of the resulting hyperbolic equations.

All the proposed algorithms and software modules have been accomplished in MATLAB environment and an ad-hoc GUI (Graphic User Interface) has also been developed to allow, in real-time, the setting and interface with the most significant variables of the system.

Finally, a checking between the TDOA estimated variance obtained through Monte Carlo simulations and those obtained by the Cramer-Rao Lower Bound (CRLB) expressions has been done, showing that the simulation results approximates to the CRLB.

II. GRAPHICAL USER INTERFACE

The GUI has been designed to simulate a controller PPI (Plain Position Indicator), the main screen capture is presented in Fig. 1. The GUI screen can be divided into several areas that have been specifically numbered in the figure. In area 1), for the current scenario, the Madrid TMA radionavigation chart is presented, here it can be appreciated the system coverage at different flight levels, the true and estimated aircraft position and the multilateration stations locations which are marked by red triangles. In area 2) the received maximum and minimum power levels at the system stations are shown. To change different simulation parameters a series of inputs controls have been placed in areas 3), 4) and 5). Finally for each aircraft, TDOA, power, DOP values and position estimation error are presented in areas 7) and 8).

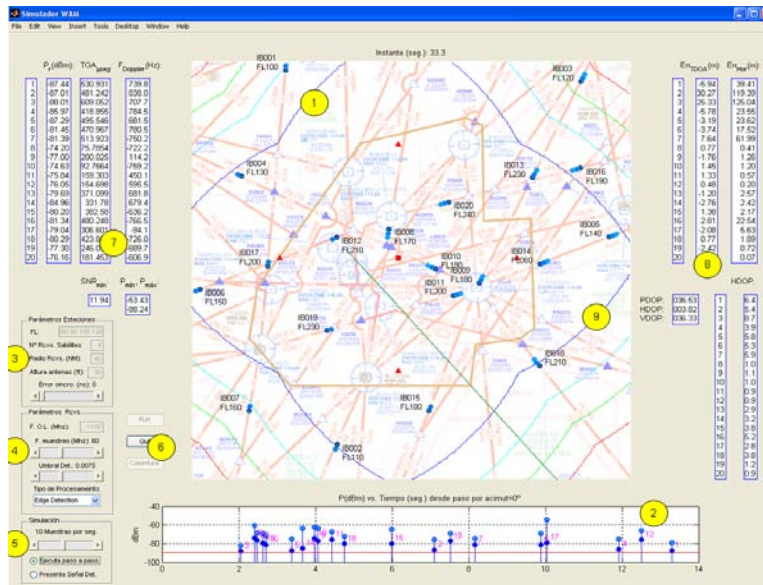


Fig. 1. GUI screen shoot.

III. WAM ARCHITECTURES

Two types of architectures based in the synchronisation method has been defined, common clock and distributed clock systems. Firstly in common clock architectures each pair of received signals is cross-correlated to produce a direct TDOA estimation measurement, the actual time of signals' arrival at the receivers are never calculated. Two algorithms types have been initially developed, one based on the cross-correlation method and another applying the ASDF (Average Square Difference Function) method.

Secondly in distributed clock architectures, all the stations clocks should be synchronized to measure the pulses edges and thus estimate the TOA (Time Of Arrival). These systems are typically used with signal waveforms on which it is easy to measure the pulse edge such as in the case of aircraft SSR transponder signals. Two algorithms types have been developed, as well, one based on the autocorrelation method using a matched filter and another using an adaptive threshold detector.

For distributed clock systems, a synchronization error software module is being developed currently, based on the GPS signal de-correlation.

IV. SSR SIGNAL SIMULATION

The WAM simulation software works with SSR mode A/C replies [1][2][3], although with additional minimum modifications the software can also work in SSR mode S. Two different input modules have been designed, one is a SSR signal generator module with a simple propagation model and the other uses transponder real signals obtained from a 1090MHz receiver.

The first module provides the signals that reach each receiving antenna [4][5]. For this purpose, an atmospheric attenuation and delay calculator have been implemented. Depending on the aircraft FL (Flight Level), the module adjusts the transponder power to PIRE=48.5dBm below FL150 (15.000 feet) and PIRE=55dBm over FL150.

Due to the long range of the system a line of sight analysis has been accomplished. The effect of the atmospheric refraction is amended using a 4R/3 value for the earth radio, to obtain the maximum range (D) in NM (Nautical Miles) at a given height (H) in feet, equation (1) has been used, where α is the energy origin angle, expressed in milliradians, and h_0 is the antenna height given in feet. Based on the free space attenuation and (1) the ranges at different flight levels have been obtained, as show in Fig. 2 a).

$$H - h_0 = \frac{2}{3} D \times (D + 9\alpha) \quad (1)$$

When the simulator works with real signals the data are obtained from a file. Due to only one receiver equipment is available, it has been necessary to record the signal from the same aircrafts at different known distances, and thus different transponder replies with different attenuation have been obtained. Adjusting the replies in time is possible to simulate the signal arrival to the different receiver stations. In Fig. 2 b) the reply from de same transponder at different distances is shown.

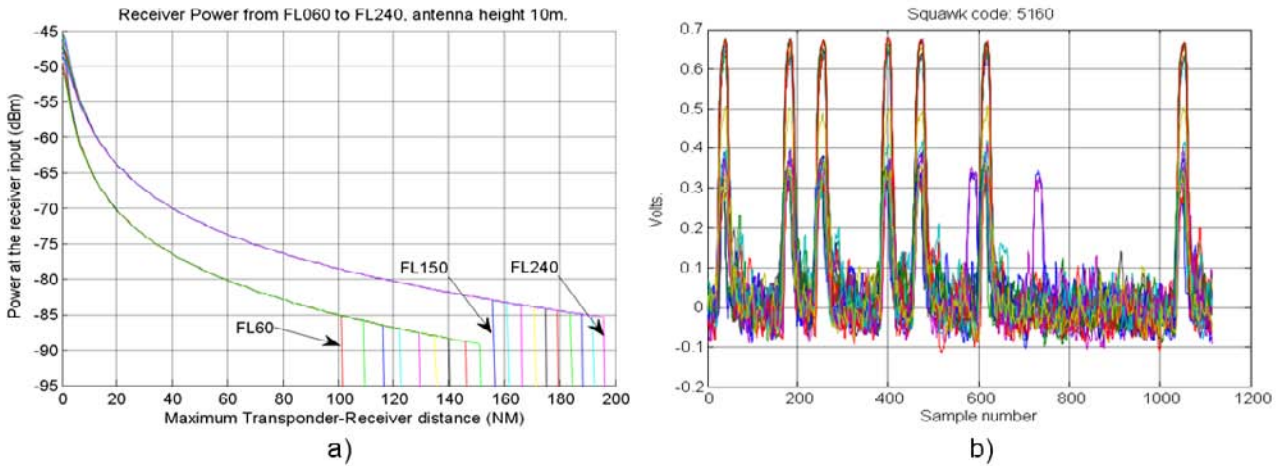


Fig. 2. a) Power at the ground stations for various FL. b) Squawk code with differents atenuations.

V. RECEIVER DESIGN

In the design of the receiver model, the types of base band processing algorithms have been taken into account [6], for this purpose a quadrature receiver has been used, as it is shown in Fig. 3, the base band signal is obtained following (2).

$$V_{BB} = \sqrt{I^2 + Q^2} \quad (2)$$

Two independent white noise generators have been used to simulate the channel and receiver noise [7]. The 10MHz IF (Intermediate Frequency) stage is digitalized by an analog to digital converter with variable sample rate between 20 MHz and 100 MHz (selected by the user).

Other receiver architectures have been analyzed as the coherent or envelope detectors, but they have been dismissed by their smaller precision on the leading edge detection of the SSR pulses.

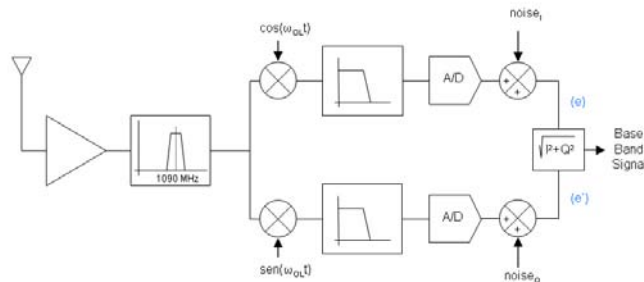


Fig. 3. Receiver block diagram.

VI. SIGNAL PROCESSING IN COMMON CLOCK ARCHITECTURES

Independently of the signal processing technique [8], a set of two receiver's base band outputs can be modelled by (3),

$$\begin{aligned} r_1[n] &= s[n] + n_1[n] \\ r_2[n] &= s[n-d] + n_2[n] \end{aligned} \quad (3)$$

where $r_1[n]$ and $r_2[n]$ are the outputs of a receivers pair, $s[n]$ is the digitalized transmitted signal, $n_1[n]$ and $n_2[n]$ represent the additive white Gaussian noises, and d is the TDOA to be estimated expressed as an integer number of samples. Two TDE (Time Delay Estimation) methods have been implemented as shown below.

A. Cross-Correlation method

One of the basic methods to compute de TDOA measurement is executing the cross-correlation between the signals received in two spatially separated ground stations. The function can be expressed as (4), since the signals and noises are assumed to be uncorrelated having zero mean and Gaussian distribution. Then, finding the maximum peak of $R_s[\tau+d]$ the estimated TDOA is obtained by (5).

$$\begin{aligned} R_{r_1r_2}[\tau] &= R\{r_1[n+\tau] \times r_2^*[n]\} = R\{r_1[n+\tau] \times s^*[n-d]\} \quad (4) \\ \hat{d} &= -\arg \max_{\tau} |R_{r_1r_2}[\tau]| \quad (5) \end{aligned}$$

In order to find fractional values of the estimated TDOA a quadratic interpolation has been accomplished, displacing the origin of coordinates the solution of the second order system can be more easily obtained, using equation (6).

$$\hat{D} = \hat{d} - \frac{1}{2} \frac{R_{r_1r_2}[\hat{d}+1] - R_{r_1r_2}[\hat{d}-1]}{R_{r_1r_2}[\hat{d}-1] - 2R_{r_1r_2}[\hat{d}] + R_{r_1r_2}[\hat{d}+1]} \quad (6)$$

B. Average Square Difference Function method

Other method that can be used in common clock architectures is the ASDF; its advantage is that it provides a good estimation for high signal to noise ratios. For a sequence of N data samples, greater than the corresponding to the sum of TDOA time and SSR signal duration, the ASDF method function can be obtained as (7). The integer estimated TDOA value can be obtained finding the minimum on the equation (7) as it is shown in (8).

$$\begin{aligned} R_{ASDF}(\tau) &= \frac{1}{N} \sum_{n=0}^{N-1} [r_1[n] - r_2[n+\tau]]^2 \quad (7) \\ \hat{d}_{ASDF} &= \arg \min_{\tau} [R_{ASDF}(\tau)] \quad (8) \end{aligned}$$

Just as in the CC (Cross-Correlation) method a quadratic interpolation is used to obtain a fractional estimated TDOA. The interpolation is necessary to obtain a better resolution than 5 meters on the estimated TDOA values working at 60 MHz sample rate.

VII. SIGNAL PROCESSING IN DISTRIBUTED CLOCK ARCHITECTURES

In this type of hardware architectures a stable time reference is present in each receiving station. Using synchronized clocks it is possible to attach a time stamp when the signal reaches each receiver. The base-band output signal at two spatially separated receivers can be modelled by (9).

$$\begin{aligned} r_1[n] &= s[n - (n_1 - n_0)] + n_1[n] \\ r_2[n] &= s[n - (n_2 - n_0)] + n_2[n] \end{aligned} \quad (9)$$

Where $r_1[n]$ and $r_2[n]$ are the receiver's pair outputs, $s[n]$ is the digitalized transmitted signal, $n_1[n]$ and $n_2[n]$ represent the additive noises, and n_0 , n_1 , n_2 are the corresponding sample number to the transmission instant and arrival times to the two receivers respectively. To eliminate the unknown n_0 value it is necessary to accomplish the difference of arrival times. For distributed clock architectures two methods have been implemented as follows.

A. Adaptive Threshold Detector method

The accomplished algorithm is based on that proposed by Torrieri [9], with some modifications in such a way that it can work in all the sample rate range. The block diagram is presented in Fig. 4.

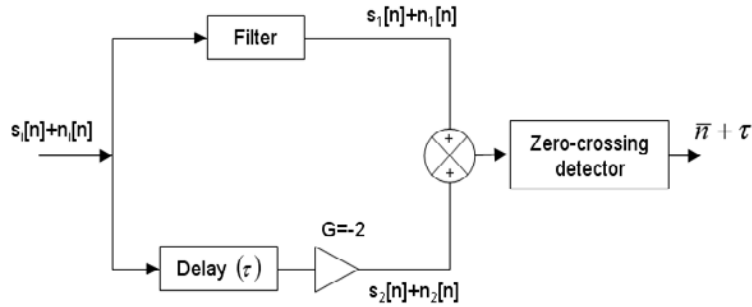


Fig. 4. ATD block diagram.

The circuit function is required to locate the middle rising edge position. The upper branch filter reduces the amplitude fluctuations on the flat portion of the SSR pulses while the signal in the lower branch is delayed until the filter output is stable. The zero-crossing of the signal at the adder output (s) is reached when the condition in (10) is achieved, at these time \bar{n} is the nearest sample number to the middle of the rising edge position. For getting a better resolution a linear interpolation has been implemented for the TOA estimation.

$$s[\bar{n} + \tau] = s_1[\bar{n} + \tau] + Gs_2[\bar{n}] = 0 \quad (10)$$

B. Matched Filter method

Matched filtering is a technique for time recovery used when the pulse shape of a signal is known, and the pulse duration is lower than the TOA. The first advantage of this technique is that SSR pulse shapes have a low-pass type frequency response, by filtering the matched filter limits the amount of the spectrum noise that is passed on to subsequent stages in the signal processing. A second advantage is that a matched filter accomplishes the auto-correlation function necessary for TOA estimation.

For a pulse amplitude of A and t_{TOA} delay, using a filter with impulse response matched to $w(t)$, the log likelihood ratio is given by (11) [10].

$$\ln \Lambda(A, \hat{\tau}) = \frac{2A}{N_0} \int_{-T}^T s(t - t_{TOA}) w(t - \tau) dt - \frac{A^2}{N_0} \quad (11)$$

where $\hat{\tau}$ is the estimated TOA and T is assumed to be much longer than the pulse period. Using (11) the estimated TOA can be expressed as (12).

$$\hat{\tau} = \arg \max_{\tau} \int_{-T}^T s(t - t_{TOA}) w(t - \tau) dt \quad (12)$$

The integral on the expression (12) represents the cross-correlation between the signals $s(t-t_{TOA})$ and $w(t)$. When the shapes of $s(t)$ and $w(t)$ are similar that integral is practically the auto-correlation function of $s(t-t_{TOA})$ [11].

The auto-correlation function can be obtained as the convolution function between $s(t-t_{TOA})$ and $h(t)$, when the impulse response of the filter $h(t)$ matches to $h(t)=w(-t)$. For the discrete base band signal at the receiver output (13) has been used, the estimated TOA value is obtained finding the maximum on $y[n]$.

$$y[n] = \sum_{k=-T}^T s[k - t_{TOA}] \cdot h_m[n - k] \quad (13)$$

In the design of the filter transfer function, the typical time values of the SSR pulses has been used, but due to the large time tolerances, an error in the maximum location of $y[n]$ is produced. These errors can reach values of up to 1.5 samples.

VIII. ALGORITHMS VALIDATION

The performance of the implemented model and that obtained based on the Cramer-Rao Lower Bound (CRLB) have been compared. A Monte Carlo simulation has been accomplished for each developed algorithm, in order to obtain the error variance and standard deviation in the TDOA and TOA estimation.

The simulations results have been compared with the variance value provided by the CRLB (Cramér-Rao Lower Bound) [12]. To this purpose it has been necessary to obtain the CRLB analytical expressions for the different WAM architectures or algorithms types.

In correlation techniques the CRLB can be expressed as indicated in (14).

$$CRLB(TDOA) = \frac{1}{8\pi^2 T^2} \int_{-\infty}^{\infty} \frac{f^2 C(f)}{1 - C(f)} df \quad (14)$$

where $C(f)$ is the squared coherence function and T the signal time duration. Manipulating (14) and considering Nyquist sampling with $f_s=2W$, yields to (15).

$$CRLB(TDOA) = \frac{3}{2\pi^2 N} \frac{1 + 2SNR}{SNR^2} \quad (15)$$

In the WAM simulator implemented to achieve greater performance the sample rate is selected over the Nyquist frequency, for a 60 MHz. sample rate the expression (15) can be adjusted to (16).

$$CRLB(TDOA) = \frac{3 \cdot 20^3}{16\pi^2 N} \frac{1 + 2SNR}{SNR^2} \quad (16)$$

Using the CRLB shown in (16) and the obtained simulation values for a sets of SNR, the standard deviation has been compared as is shown in Fig. 5.

For the ATD algorithm [13] the CRLB can be expressed as (17), where N is the noise power spectral density, τ_r , the time duration of the rising edge of the pulse and V_p the peak value of the pulse.

$$CRLB(TOA) = \sigma_{TOA}^2 \geq \frac{2N\tau_r}{V_p^2} \quad (17)$$

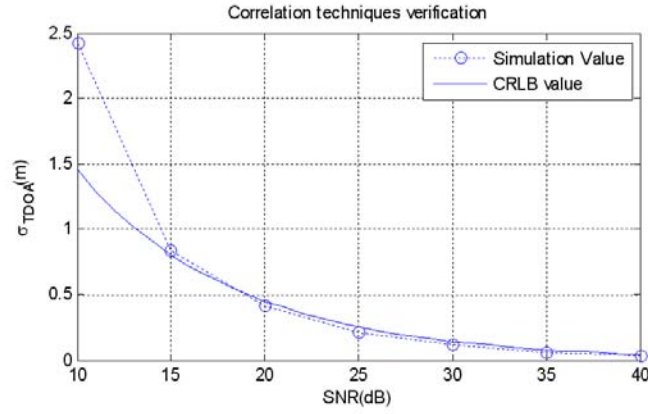


Fig. 5. Standard deviation for TDOA estimation in correlation techniques

Assuming that the accuracy at two separated receivers is similar, the standard deviation of TDOA measurements is given by (18), and the CRLB can be obtained then as (19).

$$\sigma_{TDOA} = \sqrt{2}\sigma_{TOA} \quad (18)$$

$$CRLB(TDOA) = \sigma_{TDOA}^2 \geq \frac{\tau_r^2}{SNR} \quad (19)$$

The values from the standard deviation in (19), expressed in meters, and the resulting simulation values, versus the SNR have been obtained. As show in Fig. 6, it can be proved that the simulation values are found between the theoretical values obtained for the time tolerance range of the SSR pulses.

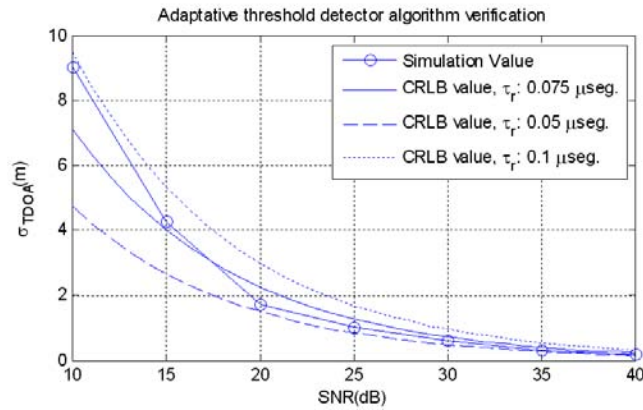


Fig. 6. Standard deviation for TDOA estimation in ATD algorithms

Finally for the matched filter algorithm [14], the CRLB takes de form in (20), and assuming (18) the standard deviation in the TDOA estimation can be obtained as (21).

$$CRLB(TOA) = \sigma_{TOA}^2 \geq \frac{1}{8\pi^2 B T_s f_c^2 SNR} \quad (20)$$

$$\sigma_{TDOA}(\text{meters}) \geq \frac{c}{2\pi B \sqrt{SNR}} \quad (21)$$

A last simulation has been accomplished to obtain the standard deviation values for matched filter algorithms, and it has been compared to the theoretical values of the expression (21), showing in Fig. 7 that the simulation results approximates to the CRLB.

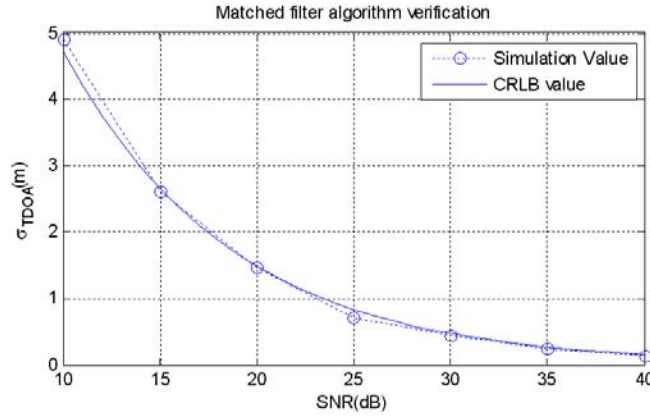


Fig. 7. Standard deviation for TDOA estimation in Matched filter algorithm

IX. LOCATION

In TDOA systems the location of a transmitter is achieved resolving a set of $N-1$ equations like the expressed in (22) [15][16][17], as can be appreciated it is considered a nonlinear system. In the presented equations $TDOA_{i,0}$ is measured between the i and 0 stations, (x_a, y_a, z_a) are the coordinates to determine and (x_0, y_0, z_0) , (x_i, y_i, z_i) are the coordinates of one central and $N-1$ remotes stations respectively.

$$c \times TDOA_{i,0} = \sqrt{(x_a - x_i)^2 + (y_a - y_i)^2 + (z_a - z_i)^2} - \sqrt{(x_a - x_0)^2 + (y_a - y_0)^2 + (z_a - z_0)^2} \quad (22)$$

To linearise the set of equations a Taylor series method has been employed. When more than three equations are used, an overdetermined system is present and a least squares method can be used to solve it. The equation (23) is solved then through an iterative process.

$$\hat{\mathbf{q}}_{k+1} = \hat{\mathbf{q}}_k + (\mathbf{F}^T \mathbf{F})^{-1} \mathbf{F}^T (\mathbf{D} - \mathbf{f}(\hat{\mathbf{q}}_k)) \quad (23)$$

In the matrix system \mathbf{q} is the coordinates vector to determine, \mathbf{D} the estimated distances differences vector and \mathbf{F} the Jacobian matrix. The positioning algorithm can be studied as a position estimator; in this case the CRLB can be calculated through the DOP (Dilution Of Precision) parameters, which over the horizontal and vertical planes can be expressed as (24).

$$\begin{aligned} \mathbf{G} &= (\mathbf{F}^T \mathbf{F})^{-1} \\ \mathbf{HDOP} &= \sqrt{\mathbf{G}_{11} + \mathbf{G}_{22}} \\ \mathbf{VDOP} &= \sqrt{\mathbf{G}_{33}} \end{aligned} \quad (24)$$

X. SYSTEM PERFORMANCES

Finally a study of system performances has been carried out, to accomplish it the covariance matrix of the position vector has been calculated for an overdetermined system, as it is indicated in (25) [18].

$$\text{cov}(d(\mathbf{q})) = (\mathbf{F}^T \mathbf{F})^{-1} \mathbf{F}^T [E\{d(\mathbf{D})d(\mathbf{D})^T\}] \mathbf{F} (\mathbf{F}^T \mathbf{F})^{-1} \quad (25)$$

Solving (25), for a grid over the system coverage, the standard deviation of the error positioning on the horizontal and vertical planes can be obtained. For a set of one central station a five remote stations uniformly distributed over a circumference and 100 NM (Nautical Milles) baselines, assuming that synchronization errors do not exists, the system accuracy obtained using (25) for a distributed architecture, using a matched filter algorithm, is shown in Fig. 8.

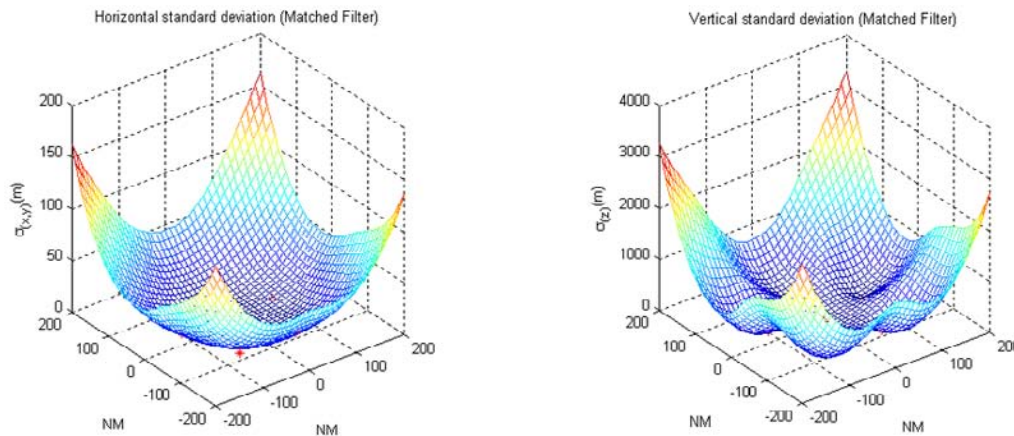


Fig. 8. Standard deviation for position estimation on horizontal and vertical planes with Matched filter algorithm

XI. CONCLUSIONS

The developed WAM simulation model is outlined as a great usefulness tool in WAM systems design. This tool permits to analyze, in a simple and rapid way, the system principal parameters, such as its coverage, signal and receiver parameters and system accuracy. Analyzing the accuracy, it has been confirmed that with correlation techniques the level of accuracy is better than the obtained with ATD or Matched filter methods. At present, we are working in a new simulator version, this one will include multipath, synchronization error estimation modules and new signal processing algorithms.

XII. REFERENCES

- [1] "Minimum Operational Characteristics for Airborne ATC Transponder Systems", RTCA/DO-144A, 2006.
- [2] "Minimum operational performance specification for Mode S multilateration use in A-SMGCS", EUROCAE, ED-177.
- [3] "Surveillance and Collision Avoidance Systems", ICAO, Annex 10 to the Convention on International Civil Aviation, Volume IV.
- [4] Andile Mngadi, "L-band RFI Measurement System Simulation and Investigation", Department of Electrical Engineering, Cape Town, February 2007, pp 26-27.
- [5] Graham Laucht, "A consideration of low power transponder systems", CAA Second draft 060706, June 2006, pp. 1-7.
- [6] Bassem R. Mahafza, Atef Z. Elsherbeni, "MATLAB Simulations for Radar Systems Design", CHAPMAN & HALL/CRC.
- [7] Herbert Taub, Donald L. Schilling, "Principles of Communication Systems", second edition, McGraw-Hill, pp 321-342.
- [8] Charles H. Knapp, G. Clifford Carter, "The Generalized Correlation Method for Estimation of Time Delay", IEEE Transactions on acoustics, speech and signal processing, vol. ASSP-24, no. 4, August 1976. pp. 320-327.

- [9] Don J. Torrieri, "The Uncertainty of Pulse Position Due to Noise", NAVAL RESEARCH LABORATORY, Washington D.C., 31 May 1972.
- [10] Chee-Cheon Chui and Robert A. Scholtz, "Estimating Parameters of Received UWB Monocycles", Asilomar Conference on Signals, Systems, and Computers, November 2004.
- [11] S. Haykin, Communication Systems, Wiley, NY, 1994.
- [12] S.M Kay, "Fundamentals of Statistical Signal Processing: Estimation Theory", London, Prentice Hall, 1993.
- [13] Aysegül Dersan, Yalçın Tanik, "Passive Radar Localization by Time Difference of Arrival", Proc. MILCOM, Anaheim (California), October 2002.
- [14] Neal Patwari, Joshua N. Ash, Spyros Kyperountas, Alfred O. Hero III, Randolph L. Moses, and Neiyer S. Correal, "Locating the Nodes", IEEE SIGNAL PROCESSING MAGAZINE, July 2005, pp. 54-69.
- [15] F. Linghan, Y. Jinrong, XuBing, M. Weirong, "Passive Location Using TDOA Measurements In Four Sites", Radar 2006. CIE '06. International Conference on, Oct. 2006, pp. 1-4.
- [16] G. Galati, M. Gasbarra, P. Magaro, P. De Marco, L. Mene, M. Pici, "New Approaches to Multilateration processing: analysis and field evaluation", Proceedings of the 3rd European Radar Conference, EuRAD 2006, pp. 116-119, Sept. 2006.
- [17] G. Galati, M. Leonardi, P. Magarò, V. Paciucci, "Wide Area Surveillance using SSR Mode S Multilateration: advantages and limitations", Radar Conference 2005, EURAD 2005, pp. 225-229, Oct. 2005.
- [18] Bradford W. Parkinson, James J. Spilker Jr., GLOBAL POSITIONING SYSTEM: THEORY AND APPLICATIONS., Volume 163 Progress in Astronautics and Aeronautics. Chapter 11, pp. 469-483.